Numerical analysis of a 155 mm artillery shell range with angular variation in trailing edge geometry

Rodrigo de Azevedo Rodrigues Paulo[1], Victor Santoro Santiago[1], André Luiz Tenório Rezende[1]

[1]Seção de Engenharia Mecânica, *IME – Instituto Militar de Engenharia,*
Praça General Tibúrcio 80, 22290-270, Rio de Janeiro, RJ, Brasil
rodrigo.azevedo@ime.eb.br, santoro@ime.eb.br, arezende@ime.eb.br

Abstract. This article aims to compare the different trajectories of a 155 mm artillery shell when changing the angle of its trailing edge, also known as boattail. To this end, an iterative numerical analysis computer program was developed where the differential equations of the projectile trajectory are solved with 4 degrees of freedom, that is, through the modified point-mass method. When solving the system of differential equations, the 4th order Runge-Kutta method is used. The trailing edge angle is a geometric characteristic that is directly related to the base drag force experienced by the ammunition. Furthermore, the magnitude of the drag force has a great influence on the firing range and this, in turn, is of great relevance for the development of a projectile. The aerodynamic coefficients are obtained using a ballistic analysis software. It generates the aerodynamic coefficients for each boattail angle as a function of Mach number. These values are then used as input data in the source code and thus the simulation can be performed. The results obtained are validated by existing data in the literature and highlight variations in trajectories, showing that the maximum range can be obtained by determining an ideal boattail angle.

Keywords: ballistics, aerodynamics, modified point-mass trajectory, Runge-Kutta method.

1 Introduction

According to Sor [1], a conventional 155 mm projectile's body generally begins with a streamlined nose and terminates using a boattail base for aerodynamic efficiency. It was popularized during the World War II era and, since then, modifications to the projectile design have been minimal. The 155 mm artillery shell is not a self-propelled projectile and thus, given the propellant charge used and the howitzer configuration, its fire range depends on its geometry characteristics.

Once in flight, the projectile is subjected to aerodynamic forces and moments in addition to gravitational acceleration. The aerodynamic drag force acts in the opposite direction of the projectile's velocity and makes a significant contribution to reducing the fire range. Sahu [2] proposed that the total drag force be divided into three components: pressure drag (excluding the base), viscous drag (skin friction), and base drag. The latter has a magnitude that can account for up to 50% of the total drag.

Base drag is caused by the wake formed in the projectile's afterbody due to the flow separation. Various techniques can be used to reduce it on a projectile in flight. The one that will be the focus of this paper is the boattail. It consists of a profile with a base diameter smaller than the body-cylinder diameter that creates a boattail angle θ_{bt} – Fig. 1 –. Suliman [3] remarks that using boattail is intended to reduce the vortex area behind the base so the strong vortex will be replaced by a smaller and a weaker one, and the low pressure will increase.

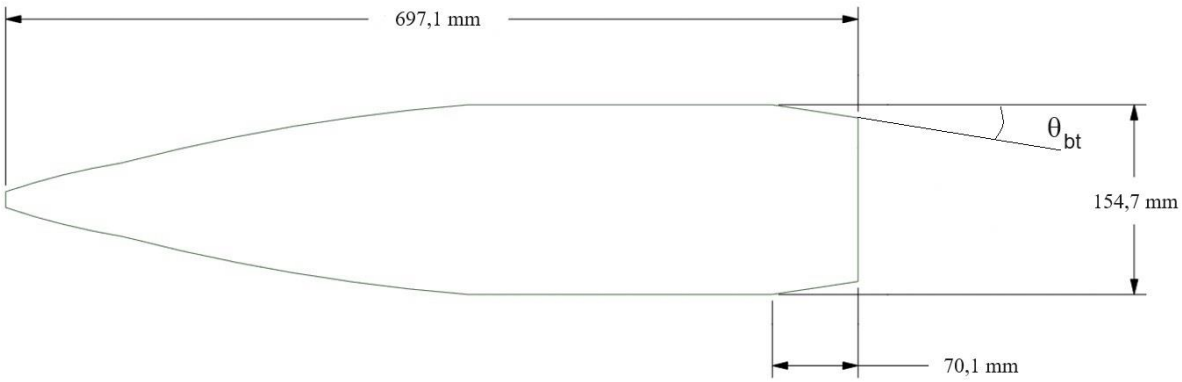

Figure 1. Geometry of a 155 mm artillery shell

The wave drag is a component of pressure drag due to compressibility effects. Although the boattail technique decreases the base drag, it increases the wave drag on the configuration. Therefore, an optimum boattail configuration results from balancing the increase in wave drag with the reduction of base drag [4]. Thus, this optimum configuration should give the longest range possible.

2 Methodology

2.1 Modified point-mass trajectory

There are several methods for formulate the equations of a projectile's trajectory, for example: the vacuum trajectory, the flat-fire point mass trajectory, the point-mass trajectory, etc. However, the six-degrees-of-freedom (6-DOF) trajectory stands out among the others for its precision. According to McCoy [5], the numerical integration of the 6-DOF differential equations of motion gives the most accurate solution possible, for the trajectory and flight dynamic behavior of a rotationally symmetric, spinning or non-spinning projectile, provided that all the aerodynamic forces and moments, and the initial conditions, are known to a high degree of accuracy.

Although the 6-DOF trajectory is very precise, the computational time required for numerical solution of the system of differential equations is large. This is due to the small integration time step required for the numerical solution to yield the high frequency epicyclic pitching and yawing motion of the projectile. A simpler formulation that has good accuracy and requires less running time is the modified point-mass trajectory (MPM). It considers this motion small everywhere along the trajectory, which is true for rotationally symmetric projectile, except in the region near the apogee for very high elevation angle of fire.

The yaw of repose is an important ballistic phenomenon that is worth explaining. The projectile axis is not perfectly aligned with its velocity vector during flight. The angle between them is called total yaw angle. Its variation with time can be understood as a sum of two movements: the first one is the yaw of repose, a quasi-steady state movement of the projectile axis off center from the trajectory direction. A spinning projectile tends to, steadily and predictably, align its axis to the yaw of repose; the second one is the epicyclic movement discussed in the previous paragraph.

The orthogonal coordinate system adopted by McCoy [5] for the movement of the projectile is used – Fig. 2 –. Its origin is placed at the gun muzzle and the axes are labeled as 1, 2 and 3. The 1 axis points downrange, the 2 axis points vertically upward and the 3 axis points to the right, when looking downrange. In addition, consider the unit vector, $\vec{x}$, that passes through the projectile's axis of rotational symmetry, directed positive from tail to nose, and the total yaw angle α_t, which is the angle between the projectile velocity vector $\vec{v}$ and $\vec{x}$.

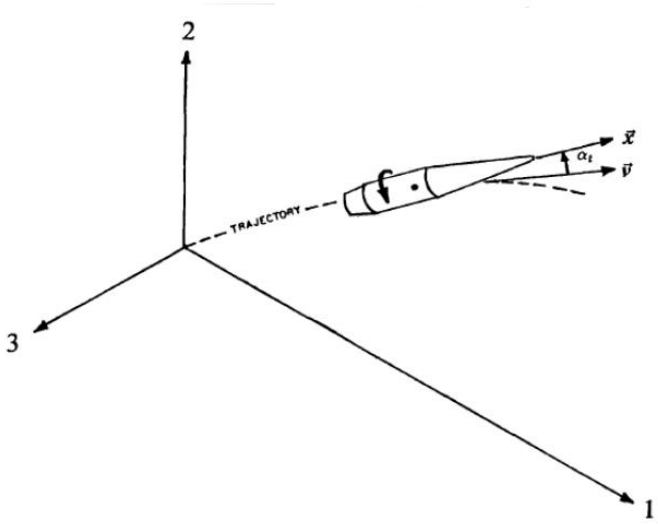

Figure 2. Coordinate system for the MPM trajectory [5]

In that way, the trajectory can be described as in the Eq. (1) to Eq. (4).

$$\frac{d\vec{V}}{dt} = -\frac{\rho A_{ref} C_D}{2m} v\vec{v} + \frac{\rho A_{ref} C_{L_\alpha}}{2m} v^2 \overrightarrow{\alpha_R} + \frac{\rho A_{ref} d C_{N_{p\alpha}}}{2m} p_x (\vec{v} \times \overrightarrow{\alpha_R}) + \vec{g} + \vec{\Lambda} \tag{1}$$

$$\frac{dp_x}{dt} = -\frac{\rho A_{ref} d^2 v}{2I_x} p_x C_{l_p} + \frac{\rho A_{ref} d v^2}{2I_x} \delta_F C_{l_\delta} \tag{2}$$

$$\overrightarrow{\alpha_R} = \frac{2I_x p_x}{\rho A_{ref} d v^4 C_{M_\alpha}} (\vec{g} \times \vec{v}) \;\; ; \;\; \vec{v} = \vec{V} - \vec{W} \;\; ; \;\; A_{ref} = \frac{\pi d^2}{4} \tag{3}$$

$$X_1(\tau) = \int_0^\tau V_1(t) dt \;\; ; \; X_2(\tau) = \int_0^\tau V_2(t) dt \;\; ; \; X_3(\tau) = \int_0^\tau V_3(t) dt \tag{4}$$

where m is the mass of the projectile, t is the time variable, ρ is the air density, I_x is the projectile axial moment of inertia, d is the projectile reference diameter ($d = 0.1547$ m), A_{ref} is the projectile reference area, $\vec{V}$ is the vector velocity of the projectile with respect to the earth fixed coordinate system, $\vec{W}$ is the wind velocity relative to the earth fixed coordinate system, $\vec{v}$ is the vector velocity of the projectile with respect to the air, v is the magnitude of $\vec{v}$, p_x is the axial spin of the projectile, $\overrightarrow{\alpha_R}$ is the vector yaw of repose, C_D is the drag force coefficient, C_{L_α} is the lift force coefficient, $C_{N_{p\alpha}}$ is the Magnus force coefficient, C_{l_p} is the spin damping moment coefficient, C_{l_δ} is the rolling moment due to fin cant, C_{M_α} is the pitching moment coefficient, δ_F is the fin cant angle, $\vec{g}$ is the vector acceleration due to gravity, $\vec{\Lambda}$ is the vector Coriolis acceleration, X_1 is the component of the projectile's displacement in the 1 direction, X_2 is the component of the projectile's displacement in the 2 direction, X_3 is the component of the projectile's displacement in the 3 direction and τ is the elapsed time since the projectile left the muzzle ($t = 0$).

2.2 Considerations for the system of equations

The 155 mm artillery shell is spin-stabilized, therefore the second term on the right side of Eq. (2) is equal to zero. The Coriolis term is very small in comparison with the acceleration of gravity, except in long range artillery fire, which is not the case in the present work, therefore $\vec{\Lambda} = 0$. The only non-null component of the vector $\vec{g}$ is $g_2 = -9.81$ m/s^2. The wind velocity is assumed to be zero, therefore $\vec{W} = 0$. By doing the substitutions on the Eq. (1) to Eq. (3) and decomposing the vectors into components (V_1, V_2 e V_3), the system of differential equations for the MPM trajectory can be written as in the Eq. (5) to Eq. (8).

$$\frac{dV_1}{dt} = -\frac{\rho A_{ref} C_D}{2m} V V_1 + \frac{I_x g_2 C_{L_\alpha}}{m d C_{M_\alpha} V^2} p_x V_3 - \frac{I_x g_2 C_{N_{p\alpha}}}{m C_{M_\alpha} V^4} p_x^2 V_1 V_2 \tag{5}$$

$$\frac{dV_2}{dt} = -\frac{\rho A_{ref} C_D}{2m} V V_2 + \frac{I_x g_2 C_{N_{p\alpha}}}{m C_{M_\alpha} V^4} p_x^2 (V_1{}^2 + V_3{}^2) + g_2 \tag{6}$$

$$\frac{dV_3}{dt} = -\frac{\rho A_{ref} C_D}{2m} V V_3 - \frac{I_x g_2 C_{L_\alpha}}{m d C_{M_\alpha} V^2} p_x V_1 - \frac{I_x g_2 C_{N_{p\alpha}}}{m C_{M_\alpha} V^4} p_x^2 V_2 V_3 \tag{7}$$

$$\frac{dp_x}{dt} = \frac{\rho A_{ref} d^2 C_{l_p}}{2 I_x} V p_x \tag{8}$$

where $V = \sqrt{V_1^2 + V_2^2 + V_3^2}$ is the magnitude of the vector $\vec{\mathrm{V}}$.

2.3 Aerodynamic coefficients

The MPM trajectory equations features five aerodynamic coefficients: C_D, C_{L_α}, $C_{N_{p\alpha}}$, C_{l_p} and C_{M_α}, being C_D given by a combination between the zero-yaw drag coefficient C_{D_0} and the yaw drag coefficient $C_{D_{\delta^2}}$ – Eq. (9). All of them are functions of the free-stream Mach number and had its values tabulated by the PRODAS ballistic analysis software. In it, it's possible to modify the boattail angle and get the changes in the aerodynamic coefficients as well as the projectile's mass and moments of inertia.

$$C_D = C_{D_0} + C_{D_{\delta^2}} sen^2 \alpha_t \tag{9}$$

2.4 Atmospheric modeling

According to the standard model of the atmosphere adopted by the International Civil Aviation organization (ICAO) [6], the atmosphere can be divided in layers where the temperature and pressure can be modeled through equations. This study approaches the fire of a howitzer. Therefore, two layers are important: ground level up to 11000 m and 11000 m up to 20000 m. Equations (10) and (11) give the equations for temperature and pressure respectively.

$$T = \begin{cases} T_0 + \beta H, & H < 11000\ m \\ 216.65, & 11000\ m \leq H \leq 20000\ m \end{cases} \tag{10}$$

$$P = \begin{cases} P_0 \left[1 + \dfrac{\beta}{T_0} H\right]^{-\frac{g_0}{\beta R}}, & H < 11000\ m \\ P_b exp\left[-\dfrac{g_0}{RT}(H - 11000)\right], & 11.000\ m \leq H \leq 20000\ m \end{cases} \tag{11}$$

where H is the altitude, $P = P(H)$ is the atmospheric pressure, $T = T(H)$ is the atmospheric temperature, T_0 and P_0 are the standard temperature and pressure at sea level ($T_0 = 288.15$ K and P_0=101325 Pa), R is the ideal gas constant for air ($R = 287.05$ J/kg·K), β is the temperature gradient ($\beta = -0.0065$ °C/m), P_b is the pressure at 11000 m of altitude ($P_b = 22632$ Pa) and g_0 is the gravitational acceleration ($g_0 = g_2 = -9.81$m/s^2).

Those equations are necessary to solve the MPM trajectory. This is because $\rho = \rho(T, P)$; in addition, the Mach number $M = M(T, P)$ determines the aerodynamic coefficients – Eq. (12) –.

$$\rho = \frac{P}{RT} \ ; \ M = \frac{V}{\sqrt{KRT}} \tag{12}$$

where K is the adiabatic expansion factor.

2.5 Runge-Kutta method

Solving the MPM trajectory requires numerical analysis. The well-known 4º order Runge-Kutta method is applied to the system of linear first order Ordinary Differential Equations presented in Eq. (5) to Eq. (8). It consists

of simple mathematic expressions and has good precision. The system of equations can then be rewritten as in Eq. (13), where the dot notation is used to represent the time derivative.

$$\begin{cases} \dot{V}_1 = f_K(V_1, V_2, V_3, p_x) \\ \dot{V}_2 = f_L(V_1, V_2, V_3, p_x) \\ \dot{V}_3 = f_M(V_1, V_2, V_3, p_x) \\ \dot{p}_x = f_N(V_1, V_2, V_3, p_x) \end{cases} \tag{13}$$

Equations (14) to (21) show how each variable can be calculated through iterative process.

$$\begin{cases} V_{1(i+1)} = V_{1(i)} + \dfrac{1}{6}[K_1 + 2(K_2 + K_3) + K_4] \\ V_{2(i+1)} = V_{2(i)} + \dfrac{1}{6}[L_1 + 2(L_2 + L_3) + L_4] \\ V_{3(i+1)} = V_{3(i)} + \dfrac{1}{6}[M_1 + 2(M_2 + M_3) + M_4] \\ p_{x(i+1)} = p_{x(i)} + \dfrac{1}{6}[N_1 + 2(N_2 + N_3) + N_4] \end{cases} \tag{14}$$

$$\begin{aligned} K_1 &= \Delta t f_K\left(V_{1(i)}, V_{2(i)}, V_{3(i)}, p_{x(i)}\right) \\ L_1 &= \Delta t f_L\left(V_{1(i)}, V_{2(i)}, V_{3(i)}, p_{x(i)}\right) \\ M_1 &= \Delta t f_M\left(V_{1(i)}, V_{2(i)}, V_{3(i)}, p_{x(i)}\right) \\ N_1 &= \Delta t f_N\left(V_{1(i)}, V_{2(i)}, V_{3(i)}, p_{x(i)}\right) \end{aligned} \tag{15}$$

$$\begin{aligned} K_2 &= \Delta t f_K\left(V_{1(i)} + \frac{K_1}{2}, V_{2(i)} + \frac{L_1}{2}, V_{3(i)} + \frac{M_1}{2}, p_{x(i)} + \frac{N_1}{2}\right) \\ L_2 &= \Delta t f_L\left(V_{1(i)} + \frac{K_1}{2}, V_{2(i)} + \frac{L_1}{2}, V_{3(i)} + \frac{M_1}{2}, p_{x(i)} + \frac{N_1}{2}\right) \\ M_2 &= \Delta t f_M\left(V_{1(i)} + \frac{K_1}{2}, V_{2(i)} + \frac{L_1}{2}, V_{3(i)} + \frac{M_1}{2}, p_{x(i)} + \frac{N_1}{2}\right) \\ N_2 &= \Delta t f_N\left(V_{1(i)} + \frac{K_1}{2}, V_{2(i)} + \frac{L_1}{2}, V_{3(i)} + \frac{M_1}{2}, p_{x(i)} + \frac{N_1}{2}\right) \end{aligned} \tag{16}$$

$$\begin{aligned} K_3 &= \Delta t f_K\left(V_{1(i)} + \frac{K_2}{2}, V_{2(i)} + \frac{L_2}{2}, V_{3(i)} + \frac{M_2}{2}, p_{x(i)} + \frac{N_2}{2}\right) \\ L_3 &= \Delta t f_L\left(V_{1(i)} + \frac{K_2}{2}, V_{2(i)} + \frac{L_2}{2}, V_{3(i)} + \frac{M_2}{2}, p_{x(i)} + \frac{N_2}{2}\right) \\ M_3 &= \Delta t f_M\left(V_{1(i)} + \frac{K_2}{2}, V_{2(i)} + \frac{L_2}{2}, V_{3(i)} + \frac{M_2}{2}, p_{x(i)} + \frac{N_2}{2}\right) \\ N_3 &= \Delta t f_N\left(V_{1(i)} + \frac{K_2}{2}, V_{2(i)} + \frac{L_2}{2}, V_{3(i)} + \frac{M_2}{2}, p_{x(i)} + \frac{N_2}{2}\right) \end{aligned} \tag{17}$$

$$\begin{aligned} K_4 &= \Delta t f_K\left(V_{1(i)} + K_3, V_{2(i)} + L_3, V_{3(i)} + M_3, p_{x(i)} + N_3\right) \\ L_4 &= \Delta t f_L\left(V_{1(i)} + K_3, V_{2(i)} + L_3, V_{3(i)} + M_3, p_{x(i)} + N_3\right) \\ M_4 &= \Delta t f_M\left(V_{1(i)} + K_3, V_{2(i)} + L_3, V_{3(i)} + M_3, p_{x(i)} + N_3\right) \\ N_4 &= \Delta t f_N\left(V_{1(i)} + K_3, V_{2(i)} + L_3, V_{3(i)} + M_3, p_{x(i)} + N_3\right) \end{aligned} \tag{18}$$

$$X_1(\tau) = X_{1(i=n)} = \frac{\Delta t}{2}\left[V_{1(i=1)} + \left(2\sum_{i=2}^{n-1} V_{1(i)}\right) + V_{1(i=n)}\right] \tag{19}$$

$$X_2(\tau) = X_{2(i=n)} = \frac{\Delta t}{2}\left[V_{2(i=1)} + \left(2\sum_{i=2}^{n-1} V_{2(i)}\right) + V_{2(i=n)}\right] \tag{20}$$

$$X_3(\tau) = X_{3(i=n)} = \frac{\Delta t}{2}\left[V_{3(i=1)} + \left(2\sum_{i=2}^{n-1} V_{3(i)}\right) + V_{3(i=n)}\right] \tag{21}$$

where Δt is the time step size for the iterations and the displacement is calculated by integration through the trapezoidal rule, being n the number of iterative steps from $t = 0$ until $t = \tau$.

3 Results

3.1 Initial conditions

The origin of the coordinate system is placed at the gun muzzle, hence $X_1(t=0) = X_{1(i=1)} = 0$, $X_2(t=0) = X_{2(i=1)} = 0$ and $X_3(t=0) = X_{3(i=1)} = 0$. In order to know the components of $\vec{V}(0)$, it is necessary to define the initial orientation of the projectile when leaving the muzzle (which, for the purpose of this work, is the same as the gun tube orientation). The angles of the gun tube from the plane 1-3 (φ_0) – elevation angle – and from the plane 1-2 (θ_0) are defined. Thus, the components of $\vec{V}(0)$ can be written as in Eq. (22).

$$\begin{aligned} V_1(0) &= V(0)\,cos(\varphi_0)\,cos(\theta_0) \\ V_2(0) &= V(0)\,sin(\varphi_0)\,cos(\theta_0) \\ V_3(0) &= V(0)\,sin(\theta_0) \end{aligned} \tag{22}$$

where $V(0) = 207.3$ m/s, $\varphi_0 = 46.3°$ and $\theta_0 = 0°$. The initial condition for the V components is, then, calculated: $V_1(0) = 143.22$ m/s, $V_2(0) = 149.87$ m/s and $V_3(0) = 0$ m/s.

Equation (23) shows how to calculate the initial axial spin rate of the projectile $p_x(0)$.

$$p_x(0) = \frac{2\pi V(0)}{rd} \tag{23}$$

where r is the rifling twist rate ($r = 20$ calibers/revolution). This gives $p_x(0) = 420$ rad/s.

3.2 Script routine validation

Once the system of ODE is complete, a script routine can be written in MATLAB R2023b to solve the MPM trajectory. However, it is necessary to validate the script before solving it. This is done by comparing the script output with the PRODAS output and with the 155 mm projectile firing table data. Both, the software PRODAS and the firing table, fix the muzzle velocity magnitude and projectile range (ΔX_1) to calculate φ_0. Then, $V(0)$ and φ_0 are used as input in the MATLAB script so the range can be calculated. The muzzle velocity magnitude is fixed at $V(0) = 207.3$ m/s. The boattail angle is the standard for the 155 mm M107 ($\theta_{bt} = 8.51°$). The results are shown in Tab. 1.

Table 1. Projectile range (ΔX_1) calculated through MATLAB script routine

PRODAS				**FIRING TABLE**			
φ_0	ΔX_1 (m)		ERROR	φ_0	ΔX_1 (m)		ERROR
(degrees)	DATA	MATLAB	(%)	(degrees)	DATA	MATLAB	(%)
3.3	500	500.5	0.10	3.3	500	500.5	0.10
6.8	1000	1001.4	0.14	6.8	1000	1002.2	0.22
1.4	1500	1501.8	0.12	10.4	1500	1504.0	0.27
14.3	2000	2002.3	0.11	14.4	2000	2004.9	0.24
18.7	2500	2502.9	0.12	18.8	2500	2505.9	0.24
23.9	3000	3003.3	0.11	23.9	3000	3004.8	0.16
30.6	3500	3504.0	0.11	30.6	3500	3501.4	0.04
42.0	3900	3905.6	0.14	41.0	3900	3893.2	0.17
46.3	3900	3906.6	0.17	47.6	3900	3890.6	0.24
57.7	3500	3512.4	0.35	57.8	3500	3501.4	0.04
64.3	3000	3022.6	0.75	64.2	3000	3034.8	1.15
69.3	2500	2540.8	1.61	68.7	2500	2607.2	4.11

It can be seen from Tab. 1 that the errors associated with the MATLAB script output are less than 1 % for most of φ_0, the exception being at the very high elevation angles of fire, as expected for MPM trajectory. The results validate the script routine so the trajectory can be calculated.

3.3 Trajectory

The MPM trajectory is calculated for eight different boattail geometries. The boattail length remains the same for all cases ($L_{bt} = 70.1$ mm) while the boattail angle varies from $\theta_{bt} = 0°$ (no-boattail) to $\theta_{bt} = 12°$ with 2° jumps. The standard boattail angle is also included for comparison ($\theta_{bt} = 8.51°$). The iterative process stops when the projectile reaches the same height as the muzzle $X_2(t) = 0$ (it should be noted that the ground is flat, with no elevations). The time step size, for good accuracy, is $\Delta t = 0.001$ s, given that computing time is not very large for this problem. Figures 3 shows the results.

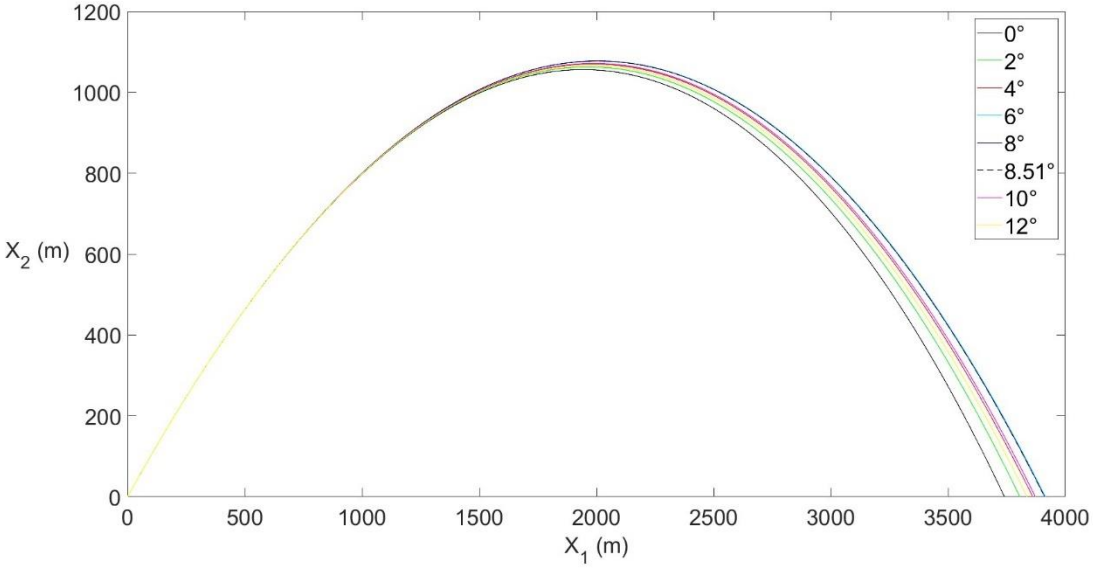

Figure 3. MPM trajectories for variable θ_{bt}

Figure 4 highlights the trajectories at the end of it.

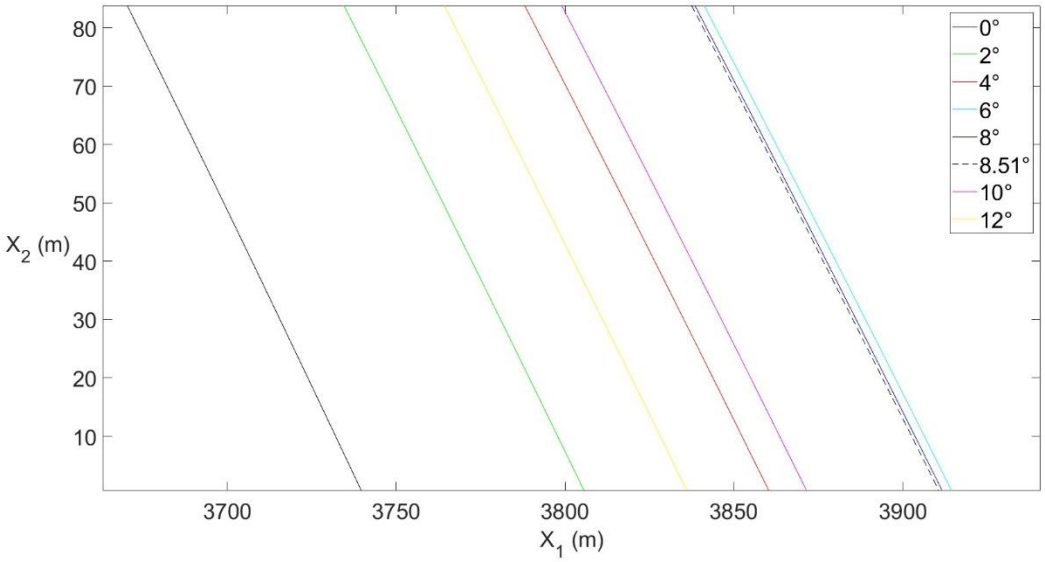

Figure 4. MPM trajectories highlights

4 Conclusion

The trajectories show an improve in range of 174.7 m (4.67 %) from the no-boattail configuration to a boattail angle of $\theta_{bt} = 6°$. It can also be noted that there is no significant difference in range from $\theta_{bt} = 6°$ to $\theta_{bt} = 8.51°$. This agrees with McCoy [5] who states that for boattail angles between 5° and 9°, the drag coefficient (as well as the others aerodynamic coefficients) vs θ_{bt} curve is relatively flat. The fact that the standard angle ($\theta_{bt} = 8.51°$) does not give the best range possible can be explained by the existence of other requirements in projectile design that were not considered in this work, however, the deviation is negligible (0.1%). The results agree with the literature on the subject.

Acknowledgements. We would like to thank the financial support provided by the Coordination for the Improvement of Higher Education Personnel (CAPES) and the Brazilian Army's Military Institute of Engineering (IME).

Authorship statement. The authors hereby confirm that they are the sole liable persons responsible for the authorship of this work, and that all material that has been herein included as part of the present paper is either the property (and authorship) of the authors, or has the permission of the owners to be included here.

References

[1] Sor, W. L. Aerodynamic validation of emerging projectile configurations. Tese (Doutorado) — Monterey, California. Naval Postgraduate School, 2012.
[2] Sahu, J.; MD., A. B. R. L. A. P. G. Drag Predictions for Projectiles at Transonic and Supersonic Speeds. Defense Technical Information Center, 1986. (Memorandum report BRL). Disponível em: <https://books.google.com.br/books?id=fAXOtgAACAAJ>.
[3] Suliman, M.; Mahmoud, O.; Al-Sanabawy, M.; Abdel-Hamid, O. Computational investigation of base drag reduction for a projectile at different flight regimes. In: THE MILITARY TECHNICAL COLLEGE. International Conference on Aerospace Sciences and Aviation Technology. [S.l.], 2009. v. 13, n. AEROSPACE SCIENCES & AVIATION TECHNOLOGY, ASAT-13, May 26–28, 2009, p. 1–13.
[4] Design of Aerodynamically Stabilized Free Rockets MIL-HDBK-762(MI) 17 July 1990.
[5] McCoy, Robert. Modern exterior ballistics: The launch and flight dynamics of symmetric projectiles. Schiffer Pub., 1999.
[6] ICAO. Manual of the ICAO Standard Atmosphere: extended to 80 kilometres. 3. ed. Montreal, 1993. 304 p.